Segmentation of Nuclei in Cancer Tissue Images: Contrasting Active Contours with Morphology-Based Approach

Santa Di Cataldo, Elisa Ficarra, Andrea Acquaviva and Enrico Macii

***Abstract*— In this paper we present a fully automated morphology-based technique for segmentation of nuclei in cancer tissue images and we compare it with a common technique for biomedical image processing, namely active contours. We discuss the limitations of active contours in the processing of immunohistochemical images characterized by heterogeneously stained nuclear region and noise caused by the presence of multiple tissue layers in the sample. We describe the integration of the proposed approach in a fully automated protein activity quantification tool. Finally, we demonstrate and motivate through extensive experiments that our fully automated morphology-based approach provides better accuracy compared to various active contours implementations.**

I. INTRODUCTION

Bio-image processing is one of the most successful and trusted research fields in that it leads to the development of diagnostic tools helping pathologists and genetists in the quantification of biological activities related to diseases [1] [2]. The overall purpose is to promote early diagnosis and to develop new therapies for multi-factorial genetic pathologies [3]. In this paper we focus on the problem of monitoring protein (i.e. the EGFR/erb-B) activity involved in the genesis and development of non-small cell lung carcinoma (NSCLC). Localization and intensity of protein activity in pathological tissues is commonly highlighted through fluorescent-marked antibodies. In this contest, the commonly used immunohistochemistry (IHC) [4] exploits intensity of stains in tissue images to quantify protein activity intensity. Image processing techniques applied to these images are devoted to the accurate and objective quantification and localization of such intensity in specific tissue regions such as cytoplasm, membranes and nuclei. Images with nuclear activations are different from images with cytoplasm/membrane activations. However, in both cases, identification of nuclear membranes is a critical step to distinguish between cellular compartments.

The main challenges in this context are related to the non predictable size, shape non uniformity induced by the pathological process and the lack of homogeneity of nuclear regions both in terms of morphological and chromatic features. From the morphological viewpoint, this is due to the overlapping of cells and nuclei and to the presence in the sample of other non pathological structures, such as connective tissue, blood vessels, lymphocytes, etc. From the chromatic viewpoint, nuclear regions are characterized by non-uniform stain intensity and color, thus preventing a trivial segmentation based on color separation. In fact, the superposition of tissue layers as well as the diffusion of the dyes on the tissue surface may bring the stains to contaminate the background or other cellular regions which are different from their specific target. Moreover, different portions of the same tissue area may be not equally enlightened and stained, thus complicating the distinction between foreground and background.

Active contours is a well known technique used in biomedical image processing [5] [6] [7] [8] [9]. In this context, remarkable intensity variations inside and outside cellular regions to be segmented stress the limitations of active contours, calling for morphology-based approaches where specific features of IHC images and other image types (e.g. fluorescent multi-channel), characterized by strong intensity and color variations within the target, can be effectively expressed and exploited.

In this paper we present a fully-automated technique that improves the accuracy of active contours in segmentation of nuclei in cancer tissue images. More specifically, the proposed approach exploits morphological information about nuclei to detect regions filled with different colors through a customized local adaptive thresholding technique. Moreover, chromatic information is exploited in our technique to separate clustered nuclei through an improved watershed algorithm.

Besides accuracy, another key metric to evaluate a bio-image processing tool is its autonomy with respect to operator input. Active contours is a semi-automated method in that it requires the operator to define a curve which the algorithm cripples iteratively to fit the boundary of the target region. On the contrary, the morphology-based technique we present in this paper provides a completely automated nuclear segmentation. Moreover, to enable fully automated procedure, we developed a pre-classification step to distinguish between images showing nuclear protein activation w.r.t. membrane and cytoplasm activation. A quantification technique for detection of protein activity in cytoplasm/membranes has been already presented in our previous paper [10]. In this work, we integrate the proposed nuclei segmentation technique in a fully automated tool for protein activity quantification in cancer tissues in all cell compartments (either membrane, cytoplasm or nuclei). A pathologist can give a set of tissue images as input to the tool which will recognize the type of activation and provide the quantification result as output.

Summarizing, the contributions of this paper are the following: i) the development of a fully automated new morphology-based technique for segmentation of nuclei with higher accuracy with respect to existing techniques; ii) the integration in a fully automated tool for protein activation

Manuscript received July 5, 2008.

S. Di Cataldo, E. Ficarra, E. Macii are with the Dep. of Control and Computer Engineering of Politecnico di Torino, Italy; A. Acquaviva is with the Dep. of Computer Science of Università di Verona, Italy.

Correspondence to santa.dicataldo@polito.it

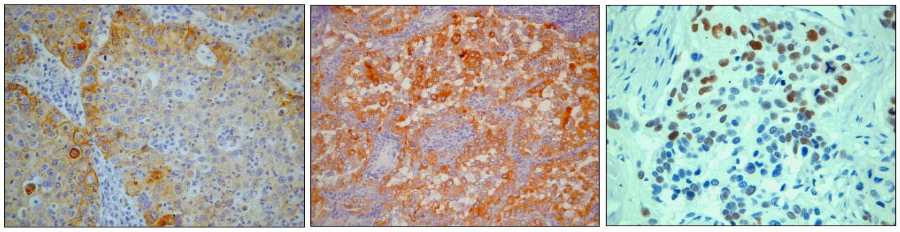

Fig. 1. IHC tissue images. From the left: membrane activations (x400); cytoplasm activations (x200); nuclear activations (x800).

quantification in cancer tissue images; iii) the comparison with various formulations of active contours technique highlighting its limitations for non-homogeneous IHC images. In particular, active contours are not suitable to handle morphological and chromatic information which is critical for this kind of images. On the other side, active contours are powerful in recognizing jagged boundaries. As such, our results open the field to the research on new approaches joining the advantages of both techniques to be applied to a wide range of biomedical images.

The paper is organized as follows. Section II explains the morphological procedure. Section III discusses contour based approaches. Section IV describes the implementation details and Section V shows experimental results. Section VI concludes the paper.

II. MORPHOLOGY-BASED PROCEDURE

In this section we present our fully-automated morphology-based procedure for nuclear segmentation in IHC tissue images. The accurate tracking of nuclear membranes is fundamental in IHC analysis. This is true not only for images with nuclear activations but also for images showing membrane as well as cytoplasm activations. In fact nuclear segmentation is usually the first step for the segmentation and quantification of protein activity of the other cellular compartments (i.e. cellular membranes and cytoplasm) [10] therefore a lack of accuracy of this step may alter IHC analysis in a substantial way.

Differently from recent methods in literature [11] our technique does not require any manual intervention by the operator, thus overcoming the subjectivity and long time-consumption of manual analysis. Moreover, our method is a comprehensive procedure able to process images with nuclear as well as with membrane or cytoplasm activity without needing any apriori knowledge about the sample. This is possible thanks to a pre-classification step that enables the automated adaptation of the procedure to the type of the image.

The images considered in this paper are characterized by blue stain (Hematoxylin, H) for highlighting the tissue structure, which represents the background. Brown stain (Diaminobenzidine, DAB) reveals protein activity. In images with membrane or cytoplasm activity only blue stain is localized in the nuclei, whereas brown stain is distributed respectively in the cellular membranes or in the cytoplasm of cells (see Fig. 1). In this paper we will refer to this category of images as Class I. In images with nuclear activations, on the contrary, both the stains are localized in the nuclei. We will refer to this category as Class II.

A. Separation of Stains

The original RGB image is separated into two monochromatic images containing respectively the contribution of the brown stain (i.e. DAB) and of the blue stain (i.e. H). For this purpose, a specific color deconvolution algorithm [12] is used, since it was shown to achieve better results than other color segmentation methods, especially in IHC applications [13]. Furthermore, it allows accurate separation not only of H and DAB but of all the standard histological stains (e.g. H-E, H AEC, etc.) as well as of any other stains, provided that their RGB vectors are experimentally determined. The color deconvolution plugin implemented by [14] was integrated to our algorithm.

B. Pre-Classification of Images

Pre-classification of the sample in Class I or II is performed by analyzing the distribution of the brown stain in the image. As shown by Fig. 1, images with nuclear activations (Class II) are characterized by a granular distribution of the brown dye and by stained regions with a well-defined round shape and nuclear-like dimension. In fact, the brown stain is always localized in the nuclei. On the contrary, in images with membrane/cytoplasm activations (Class I) brown regions are less characterized in shape and dimension: nuclear-like regions may be present again, but they are not prevalent as in Class II.

Therefore the amount of nuclear-like brown regions can be effectively used to discriminate between Class I and II. In particular, in our technique the percentage of brown pixels belonging to regions with nuclear-like shape and dimension is adopted as classification feature.

First of all, our method detects the portions of tissue stained by brown. This is achieved through automated thresholding, i.e. by imposing an intensity threshold to the brown monochromatic component and selecting pixels whose intensities are lower than the threshold. The optimal threshold is obtained through the well known Isodata algorithm [15]. Then nuclear-like particles are highlighted on the base of their shape and dimension: regions with low circularity or very small area are selectively removed.

Finally the percentage of pixels of stained tissue belonging to nuclear-like regions is calculated. Images with a low percentage (i.e. below 20%) are classified in Class I (i.e. membrane or cytoplasm activations), all the other images are classified in Class II (i.e. nuclear activations).

C. Segmentation of Nuclear Membranes.

1) Binarization: Nuclei are separated from background through automated thresholding of the monochromatic im-

ages coming from stains' separation. Since intensity level may vary among different regions of the sample because of inhomogeneous illumination and inconsistent staining, that are typical problems of IHC imaging [16], a *local adaptive threshold* [17] dependent on the local distribution of the intensities is applied. This leads to a better accuracy than traditional global thresholding. The procedure is customized through a statistical analysis of local intensity distribution. This analysis aims to minimize the effects of unrepresentative pixel values due to noise. The size of neighbourhood is selected taking into account the resolution of the image and the dimension of nuclei (for details see [18]).

For images of Class I the only contribution of the blue stain is considered to distinguish nuclei from background. On the contrary, for images of Class II both the stains are binarized and merged through binary union, thus taking into account the contribution of both the dyes.

2) Separation of Clustered Nuclei: Overlapped particles are separated through watershed algorithm [19]. As it is well known, intensity variations may lead watersheds to over-segmentation errors (i.e. to split individual nuclei in more than one particle). This problem arises especially in images with membrane/cytoplasm activations, due to the local intercontaminations of the two dyes used to highlight different cellular structures (i.e. nuclei and cellular membranes, or nuclei and cytoplasm, respectively). Unfortunately these intercontaminations occur quite often, being a consequence of the staining procedure.

In our approach over-segmentations are prevented through selective remerging of the split nuclei. First of all, the couples of particles split by watersheds are selected and the interposed area between each couple is scanned, thus computing the relative amount of blue and brown pixels. Couples of particles with a prevalence of brown pixels (i.e. belonging to cellular membrane or cytoplasm) in the interposed area are interpreted as two separated nuclei and let unchanged. On the contrary couples with a prevalence of blue pixels (i.e. belonging to nuclei) in the interposed area are interpreted as a single nucleus and remerged (see [18]).

3) Postprocessing: As already mentioned in the Introduction, the presence in the same sample of different types of tissues and cells adds a further element of complexity to the segmentation of IHC tissue images; in particular, nuclear segmentation may be led to error by lymphocytes that are usually smaller than nuclei but may appear very similar in shape and color. This problem is handled in our procedure through size analysis. Particles whose area is considerably lower than the average area of all the detected nuclei are not included in the final segmentation.

4) Extraction of Boundaries: For each detected nucleus the best-fitting ellipse is calculated and outlined. This step is aimed at improving the accuracy in the estimation of the nuclear membrane, which is typically a smooth rather than a jagged curve.

For details about parameters and implementation see Section IV.

III. ACTIVE CONTOURS APPROACH

Our morphology-based method is compared in this work with active contours, a highly popular approach in Computer Vision that was successfully used in several applications including medical imaging [20], [21]. After a general theoretical introduction, in this section we describe how we applied active contours to the segmentation of nuclear membranes in IHC images.

A. Preliminaries

Active contours (also called *snakes*) are computer-generated curves that evolve iteratively within the image from an initial position toward the boundary of the target object (i.e. the nuclear membrane, in our application) through the minimization of an energy functional [20].

This functional is generally a linear combination of: i) an *image term* E_{im} based on the characteristics of the image (e.g. gradient magnitude distribution as well as region-based statistical features), which attracts the active contour to the target boundary; ii) an *internal term* E_i based on the characteristics of the curve (e.g. tension, rigidity, etc.), which prevents the curve from interrupting or rolling up and ensures its smoothness; iii) a *constraint term* E_c defined by the user (e.g. external forces, apriori known shapes as well as points that should necessarily lie on the detected boundary). The functional is shown in the following equation

$$E_{snake}(C) = E_{im}(C) + E_i(C) + E_c(C), \tag{1}$$

where C is the evolving curve. The optimal curve $\bar{C}$ is obtained through minimization of the functional, as:

$$\bar{C} = \underset{C}{\operatorname{argmin}}\ E_{snake}(C). \tag{2}$$

Snakes are generally classified according to the curve's representation as either *parametric* active contours [20] [22] [23], where the curve in the xy plane is described explicitly in terms of a parameter t as $C(t) = (x(t); y(t))$; or *geometric* active contours [24] [25] [26], where the curve C is described implicitly as a zero level set of a higher-dimensional function f, i.e. $C : f(x,y) = 0$. Both the typologies of active contours have been successfully used for image segmentation in several applications and tasks, including medical imaging [21]. Geometric active contours are well-suited to detect objects with very elaborate shapes, however they are computationally more complex than parametric ones due to their higher-dimensional formulation and require non-trivial efforts to incorporate shape apriori information into the model [27] [28] [29] [30]. A straightforward translation from almost any parametric active contour to a geometric active contour is anyhow possible through an explicit mathematical relationship [31].

Active contours may be also classified according to the formulation of the image term guiding the evolving curve towards the target boundary as either: i) *edge-based* snakes, with image energy based on local gradient information; or ii) *region-based* snakes, with image energy based on global image information (e.g. statistical features). Edge-based snakes are generally more precise than region-based active contours: in fact the image term has sharp maxima at the gradient boundary. However region-based formulations are less sensitive to curve initialization and to noise and have less difficulties moving into concavities. Several attempts to integrate edge-based and region-based information [32] [33]

have also led to the development of *mixed* snakes, with image energy based on a combination of both the terms.

B. Parametric Spline-based Active Contour

In this work the parametric spline-based active contour presented in [22], one of the most theoretically valuable in literature, was used to segment nuclear membranes in IHC tissue images. It is based on the parametric representation of the closed curve $\mathbf{C}$ in terms of a parameter t through B-spline basis functions, as:

$$\mathbf{C}(t) = \begin{bmatrix} x(t) \\ y(t) \end{bmatrix} = \sum_{k=-\infty}^{+\infty} \mathbf{c}_k \varphi(t-k) \tag{3}$$

where $\mathbf{c}_k$ is the vector of coefficients (knot points) and φ is the basis function.

Main prerogatives of this active contour are i) cubic B-splines representation of the curve, that allows the elimination of the explicit internal energy term from the functional (1) thanks to the implicit smoothness due to minimum curvature interpolation property, and ii) a formulation of image energy as linear combination of either edge-based (taking into account gradient magnitude as well as its direction) and region-based terms, thus inheriting the advantages of both [23]. The relative contribution of the two terms can be modulated through simple variation of the coefficients, so that a general unifying framework is provided which includes all the most widely used formulations of active contours. Further details are provided in [22], [23] and [34].

C. Application to Segmentation of Nuclei in IHC Images

We developed a semi-automated procedure for the segmentation of nuclear membranes in IHC tissue images through spline-based active contours. As for our morphology-based technique, this procedure can be applied to images with nuclear activations as well as membrane or cytoplasm activations without any apriori knowledge about the image type.

The procedure consists in feeding active contours with initial boundaries manually traced by a pathologist and with a monochromatic image that provides the information needed for the calculation of the image energy term in (1). The active contours automatically converge to the final nuclear boundaries. The procedure allows the user to choose between three different active contours' formulation, respectively with *edge-based*, *region-based* and *mixed* image energy (i.e. equally weighted linear combination of edge and region-based terms). In order to perform an exhaustive comparison between active contours approach and our morphology-based method, all the three possible formulations of active contours were used in our experiments. In case the sample belongs to Class I (membrane/cytoplasm activations), image energy is calculated considering the contribution of the only blue stain. On the contrary, in case the sample belongs to Class II (nuclear activations), image energy is obtained by the contributions of both the dyes (see Section II for explanation). For this purpose the two monochromatic stains are merged together through bitwise AND operation. The techniques for pre-classification of image and separation of stains are the same used for the morphology-based approach and described in Section II.

As it is well known, one of the major drawbacks of active contours is that they are extremely sensitive to curve initialization, and they may show a lack of convergence far away from the target boundary [21]. For this reason, in order to obtain the best performance achievable, the operator was asked to trace the initial curves very close to the nuclear membranes. An example is shown in Fig. 2, where the red curves are the initial boundaries traced by the operator close to the nuclear membranes and the black curves are the final boundaries obtained through active contours approach. The parameters of the active contours (e.g. knot spacing, etc.) were tuned by running experiments on real IHC images and are provided in our URL [35].

IV. IMPLEMENTATION

The procedures were implemented in Java as plugins for ImageJ [36], a public domain software for image analysis and processing. We inherited the whole class hierarchy of ImageJ 1.38 API and the open-source plugins and macros for color deconvolution, local thresholding and spline-based snakes [14], [37], [34] and we implemented our own functions and classes. The parameters of both the methods were set by running experiments on real IHC images. See our URL [35] and [18] for details.

V. EXPERIMENTAL RESULTS AND DISCUSSION

Our morphology-based method and the active contours approach were compared on the same real IHC images, on more than 900 nuclei. These images showed lung cancer tissue stained by H-DAB and were acquired through high resolution confocal microscopy with three different enlargements (x200, x400 and x800). Ten different histological samples were used to take the pictures: five of these samples showed activations of the target protein in the cellular membrane of the cancerous cells, two in the cytoplasm and the remaining three in the nuclei (see Fig. 1 for some examples).

The morphology-based method did not require any manual intervention by the user, since it is fully-automated, whereas active contours had to be manually initialized by a skilled operator by tracing boundaries very close to the target nuclear membranes (see Fig. 2), thus leading the active contours to the best performance achievable.

In order to perform an exhaustive comparison, experiments were run with three active contours, with different formulations of the image energy functional, i.e. respectively edge-based, region-based and mixed (with equally weighted linear combination of edge and region-based terms [35]).

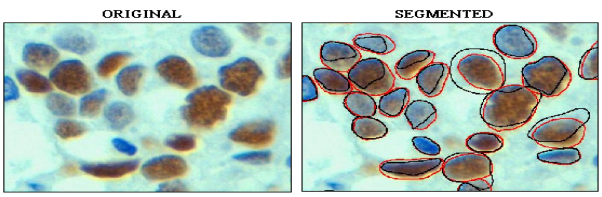

Fig. 2. Example of active contours' segmentation (manual initial boundaries in red, final converged active contours in black). Despite they are initialized very close to the target nuclear membranes, several examples of lack of convergence of active contours are clearly visible in the segmented image.

We evaluated the accuracy of the segmentations performed by both the automated and the semi-automated methods through a very strict pixel-wise comparison with reference nuclei provided by manual operators; this procedure was repeated for each of the 900 nuclei in our validation dataset; then the tested methods were compared with each other by calculating: i) the mean accuracy achieved in the validation dataset; this allows to estimate the quality of nuclear segmentation achievable on average by each of the tested methods and to deduce which is statistically the best; ii) the percentage of nuclei in which the best technique overcome the accuracy of other techniques; this adds meaningfulness to the previous result, being a measure of the recurrence of the superiority of the best technique over other methods (in fact average accuracy may be biased by few non-representative critical instances).

Segmentation accuracy was estimated as

$$Accuracy(\%) = 100 \cdot \left[1 - \frac{\sum(R \text{ XOR } A)}{\sum(R \text{ OR } A)}\right], \qquad (4)$$

where R is a binary image where pixels belonging to the reference manual nucleus are set to 1 and A is a binary image where pixels enclosed by the nuclear boundary provided by the automated (or semi-automated) procedure are set to 1. As shown by Fig. 3, R XOR A returns the pixels that were misclassified by the automated method (i.e. non-nuclear pixels classified as nuclear and vice-versa) whereas R OR A returns the totality of the evaluated pixels: therefore accuracy is the complementary of the percentage of misclassification.

Manual segmentation may lack reproducibility [11] due to the critical characteristics of IHC tissue images (e.g. small dimension of nuclei, superposition of cells and tissues, heterogeneity of staining, intercontamination of dyes, etc.). To improve the objectivity of our validation for each nucleus ten skilled operators were asked to outline manually the nuclear membrane. Thereafter, the reference nucleus used for the validation was defined by only those pixels enclosed by the most part of the ten manual boundaries.

Morphology-based method achieved on average an 84% accuracy, overcoming mean accuracy of edge-based, mixed and region-based active contours of respectively 10%, 12% and 14%; these values were obtained by averaging the accuracy achieved in all the tested nuclei. The graph of Fig. 4 shows mean accuracy values obtained grouping results according to the type of the sample (i.e. with membrane, cytoplasm or nuclear activations): the morphology-based technique achieved the best accuracy at all times. Despite they were manually initialized very close to the target boundaries, all the three formulations of active contours tested in our experiments were overcome by our fully-automated procedure.

It must be noted that edge-based snakes performed slightly

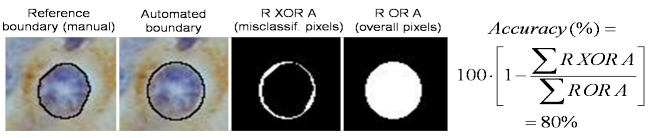

Fig. 3. Calculation of segmentation's accuracy. Example.

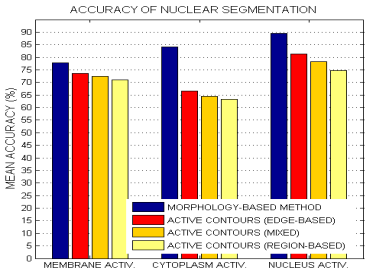

Fig. 4. Mean percentage accuracy achieved by respectively morphology based procedure, edge-based, mixed and region-based active contours in validation samples with membrane, cytoplasm or nuclear activity.

better than region-based snakes mainly because the initial curve drawn by the skilled operator is very well fitting to the nuclear membrane. However, active contours still fails in detecting nuclear regions in presence of intensity gradients inside the region. Moreover, it is well known that edge-based snakes are the most sensitive to curve initialization [22], so they might have lacked convergence if the initial curve had not been so close to the nuclear membrane as it was in our experiments. Region-based active contours are less sensitive to gradients, however this technique also fails when nuclei are characterized by non-homogeneous staining. Moreover, because it is based on statistical characterization of background, its performance is worse when images contain heterogeneous regions with different distribution and density of nuclei. The main reasons for the superiority of the morphology-based approach we propose lies in the *binarization* step and separation of clustered nuclei. The *binarization* step handles the heterogeneity of staining and the consistent intensity variations within the target through the adaptive local thresholding algorithm. The local nature of this approach enables a better distinction between the colored nuclear regions and the background. As a result, regions are successfully identified even if they are characterized by intensity variations and heterogeneous staining. On the other side, the enhanced watershed algorithm exploits color information to merge oversegmented nuclei compared to active-contours that take gray-scale images as input. RGB versions of active contours [5] [9] suffer from similar limitations in that they cannot handle heterogeneous stained local regions. Ultimately we found out that active contours are in general not expressive enough to handle complex and heterogeneous chromatic information in IHC, where the targets cannot be distinguished by simple color/texture features. Therefore a correct segmentation requires high-level interpretation of the biological information carried by color, which is actually not provided by any available active contours formulation.

The second test we performed (i.e. nucleus by nucleus comparison) showed that our technique was more performing than active contours in the most part of the nuclei of the validation dataset: in fact its accuracy was higher than edge-based, mixed and region-based active contours' accuracy respectively in 65%, 66% and 67% of the evaluated nuclei.

Fig. 5 shows examples of nuclear segmentations performed by the tested techniques (most evident errors made by active contours are highlighted in red).

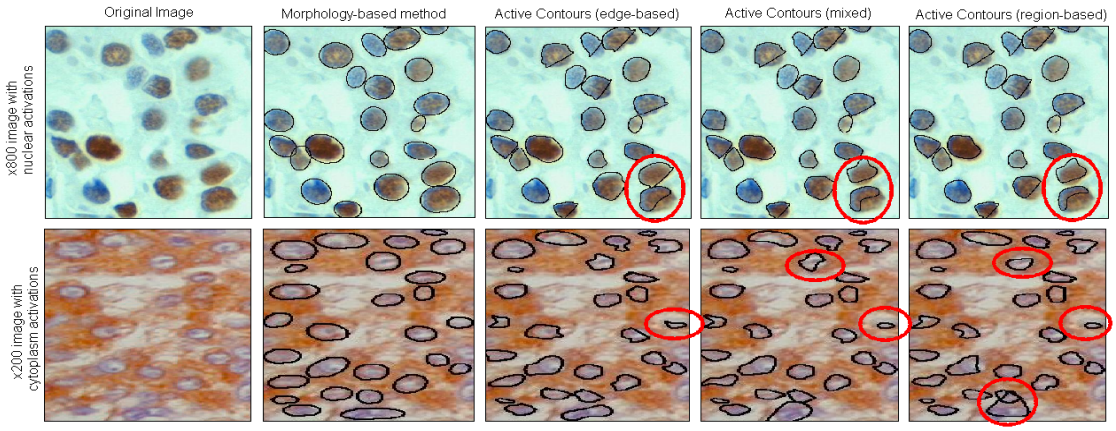

Fig. 5. Examples of nuclear segmentations performed by the tested methods. Most evident errors made by active contours are highlighted in red.

VI. CONCLUSIONS

In this paper we compared the effectiveness of a morphology-based and active contours approaches to nuclei segmentation. The experimental results show that our fully-automated morphology-based technique performs better nuclear segmentations than various formulation of state-of-the-art semi-automated active contours approach in IHC tissue images. Morphology-based strategy is less sensitive to intensity and color variations within the target region as well as overlapped nuclei that deviate the active contours far from the target. As a future work, we are going to extend our morphology-based technique to other types of biomedical images, including 3D applications.

VII. ACKNOWLEDGMENTS

The authors would like to acknowledge the pathologists of Hospital S.Luigi, Orbassano, Torino for providing the images used in the experiments as well as for the helpful discussions.

REFERENCES

[1] A. Hengerer et al., From Genomics to Clinical Molecular Imaging, *in Proc. of IEEE* Vol.93:4, 2005.
[2] W. Chen et al., Unsupervised tissue microarray analysis for cancer research and diagnostics, *IEEE T Inf Technol B* Vol.8:2, pp. 89-96, 2004.
[3] T.K.Taneja et al., Markers of small cell lung cancer, *World J Surg Oncol*, Vol.2:10, 2004.
[4] J.T. Jrgensena et al., Pharmacodiagnostics and Targeted TherapiesA Rational Approach for Individualizing Medical Anticancer Therapy in Breast Cancer, *The Oncologist*, Vol.12:4, pp. 397-405, 2007.
[5] L. Yang et al., Unsupervised segmentation based on robust estimation and color active contour models, *IEEE T Inf Technol B*, Vol.9:3, pp. 475-486, 2005.
[6] D.P. Mukherjee et al., Level set analysis for leukocyte detection and tracking, *IEEE T Image Process*, Vol.13:4, pp. 562-572, 2004.
[7] A. Elmoataz et al., Using active contours and mathematical morphology tools for quantification of immunohistochemical images, *Signal Processing*, Vol.71:2, pp. 215-226, 1998.
[8] A. Garrido et al., Applying deformable templates for cell image segmentation, *Pattern Recognition*, Vol.33:5, pp. 821-832, 2000.
[9] Ling Pi, Color Image Segmentation for Objects of Interest with Modified Geodesic Active Contour Method, *J Math Imaging Vis*, Vol.27:1, pp. 51-57, 2006.
[10] E. Ficarra et al., Computer-Aided Evaluation of Protein Expression in Pathological Tissue Images, *in Proc. of CBMS'06*, Salt Lake City, Utah, US, 2006, pp 413-418.
[11] M. Lejeune et al., Quantification of Diverse Subcellular Immunohistochemical Markers with Clinicobiological Relevancies: Validation of a New Computer-Assisted Image Analysis Procedure, *J Anat*, Vol. 212:6, 2008, pp 868-878.
[12] A.C. Ruifrok et al., Quantification of Histochemical Staining by Color Deconvolution, *Anal Quant Cytol Histol*, Vol. 23:4, 2001, pp 291-299.
[13] A.C. Ruifrok et al., Comparison of Quantification of Histochemical Staining by Hue-Saturation-Intensity (HSI) Transformation and Color Deconvolution, *Appl Immunohisto M M*, Vol.11:1, 2004, pp 85-91.
[14] G. Landini, "Software", October 2007, http://www.dentistry.bham.ac.uk/landinig/software/software.html
[15] T.W. Ridler et al., Picture Thresholding Using an Iterative Selection Method, *IEEE T Syst M Cy*, SMC-8, 1978, pp 630-632.
[16] T.W. Nattkemper, Automatic Segmentation of Digital Micrographs: a Survey, *in Proc. of MEDINFO'04*, Vol.11(Pt 2), San Francisco, CA, US, 2004, pp 847-851.
[17] N. Milstei, Image Segmentation through Adaptive Thresholding, *Technion - Israel Institute of Technology*, 1998, pp 1-38.
[18] S. Di Cataldo et al., Selection of Tumor Areas and Segmentation of Nuclear Membranes in Tissue Confocal Images: A Fully Automated Approach, *in Proc. of BIBM'07*, Fremont, CA, US, 2007, pp 390-398
[19] J. Roerdink et al., The Watershed Transform: Definitions, Algorithms and Parallelization Strategies, *Fund Inform*, Vol. 41, 2001, pp 187-228.
[20] M. Kass et al., Snakes: active contours models, *Int'l J Comp Vis*, Vol. 1(4), 1987, pp 321-331.
[21] T. McInerney et al., Deformable Models in Medical Image Analysis: A Survey, *Med Image Anal*, Vol. 15(6), 1993, pp 580-591.
[22] M. Jacob et al., A Unifying Approach and Interface for Spline-based Snakes, *in Proc. of SPIE MI*, Vol. 4322, 2001, pp 340-347.
[23] M. Jacob et al., Efficient Energies and Algorithms for Parametric Snakes, *IEEE T Image Process*, Vol. 13(9), 2004, pp 1231-1244.
[24] V. Caselles et al., Geodesic Active Contours, *in Proc. 5th Int. Conf. Computer Vision*, Boston, MA, US, 1995, pp 694-699.
[25] T. Chan et al., Active Contours without Edges, *IEEE T Image Process*, Vol. 10, 2001, pp 266-276.
[26] S. Osher et al., Fronts Propagating with Curvature-dependent Speed: Algorithms Based on Hamilton-Jacobi Formulations, *J Comput Phys*, Vol. 79, 1988, pp 12-49.
[27] M.E. Leventon et al., Statistical Shape Influence in Geodesic Active Contours, *in Proc. of CVPR'00*, Vol. 1, 2000 pp 316-323.
[28] Y. Chen et al., Using Prior Shapes in Geometric Active Contours in a Variational Framework, *IJCV*, Vol. 50:3, 2002, pp 315328.
[29] M. Rousson et al., Shape Priors for Level Set Representations, *in Proc of ECCV*, Copenhagen, 2002, pp 78-92.
[30] F. Huang et al., Face Contour Detection Using Geometric Active Contours, *in Proc. of WCICA'04*, Shanghai, 2002, pp 2090-2093.
[31] C. Xu et al., On the Relationship between Parametric and Geometric Active Contours, *in Proc. of Asilomar'00*, 2000, pp 483-489.
[32] N. Paragios et al., Unyfing Boundary and Region-based Information for Geodesic Active Tracking, *in Proc. IEEE CVPR*, Forth Collins, CO, US, 1999, pp 300-305.
[33] S.C. Zhu et al., Region Competition: Unifying Snakes, Region Growing, and Bayes/MDL for Multiband Image Segmentation, *IEEE T PAMI*, Vol. 18, 1996, pp 884-900.
[34] M. Jacob, http://bigwww.epfl.ch/jacob/software/SplineSnake.
[35] http://santa.dicataldo.googlepages.com/bibe-parameters
[36] W.S. Rasband, ImageJ, U. S. National Institutes of Health, Bethesda, Maryland, USA, http://rsb.info.nih.gov/ij/.
[37] R. Couture, http://www.aecom.yu.edu/aif/instructions/imagej/macros/local-threshold-unsharp-masking.txt.